

# Estimation of the influence of grid resolution on the results of numerical simulation the flow around a high-speed aircraft

O. A. Pashkov<sup>1\*</sup> and B. A. Garibyan<sup>1</sup>

<sup>1</sup>Moscow Aviation Institute (National Research University), 4, Volokolamskoe Shosse, Moscow, 125993, Russia

**Abstract.** The most important step in the correct solution of discrete analogs of the equations of gas dynamics for the high-speed flow of a compressible chemically active gas using grid methods is to ensure sufficient grid resolution of regions with high gradients of gas-dynamic parameters, that is, the region of the departed curvilinear shock wave compressed and boundary layer. In this work, the grid independence of the main flow parameters on the dimensionality of the computational grid was checked on the problem of flowing a sphere by a high-speed flow of a gas mixture. The dependences of gas-dynamic flow parameters on the grid resolution along the normal to the sphere surface are revealed. The conclusions about the sufficiency of the grid resolution for a particular problem have been made.

## 1 Introduction

Among the tasks facing modern science, one of the most important is the task of the most accurate prediction of the parameters of heat and mass exchange on the surfaces of high-speed atmospheric aerial vehicles at the stage of their design. The successful solution to this problem will allow optimizing its trajectory, geometric, weight, and layout parameters already at the stage of design, and, accordingly, to form requirements for the thermal protection of the vehicle, as well as to choose the composition of the necessary materials for this purpose, based on the study of their properties [1-53]. For high-speed aircraft, it is especially important to determine the thermal conditions of such most heat-stressed surface areas as the fuselage nose, leading edges of wings, edges of inlet devices, etc., which, as a rule, have the shape of blunted bodies.

Depending on the speed of the aircraft flight is accompanied by a certain degree of intensity of aerodynamic heating of its surface. In the process of such heating, the temperature of the most heat-stressed elements of the aircraft structure can exceed the maximum permissible, which threatens the destruction of the entire aircraft structure.

The most important step in solving the discrete analogs of the gas dynamics equations for a high-speed airflow is to provide sufficient grid resolution of areas with high gradients of gas-dynamic parameters. Within the framework of this work, studies of the grid

---

\* Corresponding author: [nbulychev@mail.ru](mailto:nbulychev@mail.ru)

independence of the solution of the gas dynamics equations and determination of the main criteria for the sufficiency of the grid model were carried out on the problem of flowing around a sphere.

It should be noted that the work did not aim to check the overall reliability of the results obtained, as this issue requires a separate study of the mechanisms of chemical kinetics, radiant heat transfer, etc. The mathematical model used in this work, based on the solution of the system of Navier-Stokes equations discretized by the finite volume method for the model of five-component ( $N_2$ ,  $O_2$ ,  $N$ ,  $O$ ,  $NO$ ) chemically nonequilibrium air, has been described in detail and tested on a large number of blunt bodies at different parameters of the incoming flow [54-60]. At the same time, the dependence of the accuracy of the obtained results on the number of solution iterations, and the computational grid thickening parameters was evaluated [61]. The accuracy criterion, in this case, is the energy integral.

## 2 Task statement

The analysis of the influence of the computational grid structure on the accuracy of simulation results was carried out during the study of heat and mass transfer processes when a high-speed gas mixture flow flows around the frontal part of the sphere with radius  $R = 0.03048$  m. In this case, the sphere should be perceived as a blunted part of the heat-stressed element of the aircraft, rather than as an independent aircraft. The speed of the incoming flow corresponded to the Mach number  $M_\infty = 29,45$ , parameters of the incoming flow: temperature – 196.7 K, pressure – 12.21 Pa taken from the work [62]. In all calculations, it was assumed that the sphere has a wall with temperature  $T_w = 300$  K, and infinite catalytic activity  $k_w \rightarrow \infty$ .

The grid independence of the solution was investigated on two-dimensional structured computational meshes, which have certain advantages over unstructured meshes when modeling high-speed flows [63]. To save computational resources, the problem was solved in the axisymmetric formulation, i.e. it was assumed that the flow is identical in all meridional sections of the sphere, which allowed modeling in only one section.

The effect of changing the size of the cells along the normal to the sphere surface on the flow parameters along the normal to the breaking point was investigated on the computational grids, the parameters of which are presented in Table 1. At the same time, the size of the computational domain and the block structure remained unchanged.

**Table 1.** Parameters of computational grids.

Mesh number	Mesh dimensions	Number of cells
1	40 x 80	3200
2	60 x 80	4800
3	80 x 80	6400
4	100 x 80	8000
5	120 x 80	9600

As an example, Figure 1 shows a computational grid No. 1 of size 40x80 cells with the coordinate system applied to it. The breaking point is taken as the origin of the coordinate system, and the abscissa axis coincides with the velocity vector of the incoming flow.

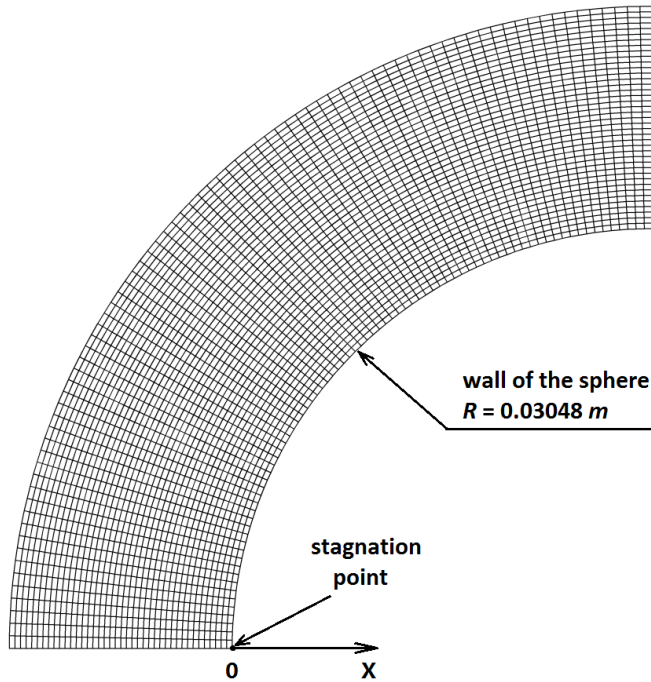


Fig. 1. The computational grid of 40x80 cells.

### 3 Properties of the components of the air mixture

Air was considered a mixture of five components:  $N_2$ ,  $O_2$ ,  $NO$ ,  $N$ ,  $O$ .

The density of the mixture as a function of pressure and temperature was calculated using the ideal gas formula:

$$\rho_{cm} = \frac{P_{ct}}{R_{\mu} T \sum_i \frac{C_i}{M_i}}, \quad (1)$$

where  $P_{ct}$  – local static pressure;  $R_{\mu} = 8,314 \text{ J} / (\text{K} \cdot \text{mol})$  – universal gas constant;  $T$  – local static temperature;  $C_i$  – mass concentration of the  $i$ -th component;  $M_i$  – a molar mass of the  $i$ -th component;

The specific isobaric heat capacity  $c_{p,i}$  of each  $i$ -th component was set by the piecewise linear law as a function of temperature [64].

The average specific heat capacity of the gas mixture was calculated using the ratio:

$$c_{p,cm} = \sum_{i=1}^n C_i \cdot c_{p,i}, \quad (2)$$

where  $c_{p,i}$  – specific isobaric heat capacity of the  $i$ -th component.

The thermal conductivity coefficient  $\lambda_i$  of each  $i$ -th component was calculated using the relation from the kinetic theory of gases [65]:

$$\lambda_i = \frac{15 R_\mu}{4 M_i} \cdot \mu_i \left[ \frac{4 c_{p,i} M_i}{15 R_\mu} + \frac{1}{3} \right], \quad (3)$$

where  $M_i$  – a molar mass of the  $i$ -th component;  $\mu_i$  – dynamic viscosity of the  $i$ -th component, function  $\mu_i(T)$ ;  $c_{p,i}$  – specific isobaric heat capacity of the  $i$ -th component.

The thermal conductivity of the gas mixture was calculated using the ratio:

$$\lambda_{\text{cm}} = \sum_{i=1}^n C_i \cdot \lambda_i, \quad (4)$$

where  $\lambda_i$  – heat transfer coefficient of the  $i$ -th component [64].

The dynamic viscosity of each component was calculated as a function of static temperature according to the well-known Blottner correlation [66], and then the dynamic viscosity of the gas mixture was calculated:

$$\mu_{\text{cm}} = \sum_{i=1}^n C_i \mu_i, \quad (5)$$

where  $\mu_i$  – dynamic viscosity of the  $i$ -th component [66];

The molar masses of all components, entropy, and enthalpy values under normal conditions ( $P = 101325 \text{ Pa}$ ,  $T = 298.15 \text{ K}$ ) are taken from [64].

## 4 Chemical kinetics

Taking into account the characteristic flow times and chemical processes, the model of nonequilibrium chemistry was used in modeling. A model consisting of five basic non-equilibrium chemical dissociation-recombination reactions was used, three of which are realized with the participation of third bodies (M) (Table 2).

**Table 2.** Major nonequilibrium chemical reactions.

1	$\text{O}_2 + \text{M} \leftrightarrow 2\text{O} + \text{M}$
2	$\text{N}_2 + \text{M} \leftrightarrow 2\text{N} + \text{M}$
3	$\text{NO} + \text{M} \leftrightarrow \text{N} + \text{O} + \text{M}$
4	$\text{N}_2 + \text{O} \leftrightarrow \text{NO} + \text{N}$
5	$\text{NO} + \text{O} \leftrightarrow \text{O}_2 + \text{N}$

For each of the components of the gas mixture, a separate mass transfer equation was solved as:

$$\frac{\partial}{\partial t} (\rho_i C_i) + \nabla \cdot (\rho_i u C_i) = -\nabla \cdot \mathbf{g}_i + \omega_i \quad (6)$$

where  $\mathbf{g}_i$  – diffusion flux of the  $i$ -th component;  $\omega_i$  – the rate of formation of the  $i$ -th component in chemical reactions;

The velocity  $\omega_i$  was calculated by the formula:

$$\omega_i = M_{w,i} \sum_{r=1}^{N_R} \hat{R}_{i,r}, \quad (7)$$

where  $M_{w,i}$  – a molar mass of the  $i$ -th component;  $N_R$  – the number of chemical reactions involved in the process and the calculation;  $\hat{R}_{i,r}$  – is the molar rate of formation (decay) of the  $i$ -th component in reaction  $r$ , calculated using the chemical kinetics equation for the rate of formation of the  $i$ -th component during a nonequilibrium chemical reaction.

The molar rate of formation (decay) of the  $i$ -th component in the nonequilibrium chemical reaction  $r$ , was represented as:

$$\hat{R}_{i,r} = \Gamma(v''_{i,r} - v'_{i,r}) \left( k_{f,r} \prod_{j=1}^N [X_{j,r}]^{\eta'_{j,r}} - k_{b,r} \prod_{j=1}^N [X_{j,r}]^{v''_{j,r}} \right), \quad (8)$$

where  $X_{j,r}$  – is the molar concentration of component  $j$  in the reaction  $r$  (Kmol/m<sup>3</sup>);  $\eta'_{j,r}$  – degree index for reagent  $j$  in the reaction  $r$ ;  $v'_{j,r}$  – the stoichiometric coefficient for reagent  $j$  in the reaction  $r$ ;  $v''_{j,r}$  – the exponent for product  $j$  in reaction  $r$  (always equal to the stoichiometric coefficient of the reaction product);  $\Gamma$  – coefficient taking into account the effect of third bodies on the reaction rate;  $k_{f,r}$  – rate constant of direct reaction;  $k_{b,r}$  – rate constant of the reverse reaction.

The rate constant of each direct reaction  $r$  was calculated using the Arrhenius expression:

$$k_{f,r} = A_{f,r} T^{\beta_{f,r}} e^{-E_{f,r}/R\mu T},$$

where  $A_{f,r}$  – pre-exponential factor;  $\beta_{f,r}$  – temperature index;  $E_{f,r}$  – reaction activation energy.

The empirical coefficients involved in the Arrhenius expression for the direct reaction and the efficiency values of each chemical component as a third body were refined from [63].

The rate constant of the reverse reaction  $k_{b,r}$  in equation (8) was calculated through the Gibbs free energy change [67].

## 5 Analysis of the results

In the course of the calculations, it was found that a decrease in the cell size along the normal to the sphere surface at the point of braking leads to a refinement of the thermodynamic parameters of the shock wave.

Figures 2 - 4 show the distribution of the dimensionless static temperature  $\bar{T} = T/T_\infty$ , density  $\bar{\rho} = \rho/\rho_\infty$  and excessive static pressure  $\bar{P} = P/(\rho_\infty \cdot V_\infty^2)$  along the normal to the surface of the sphere at the braking point. On the abscissa axis the dimensionless coordinate  $\bar{X} = X/R$ , where  $R$  – the radius of the sphere.

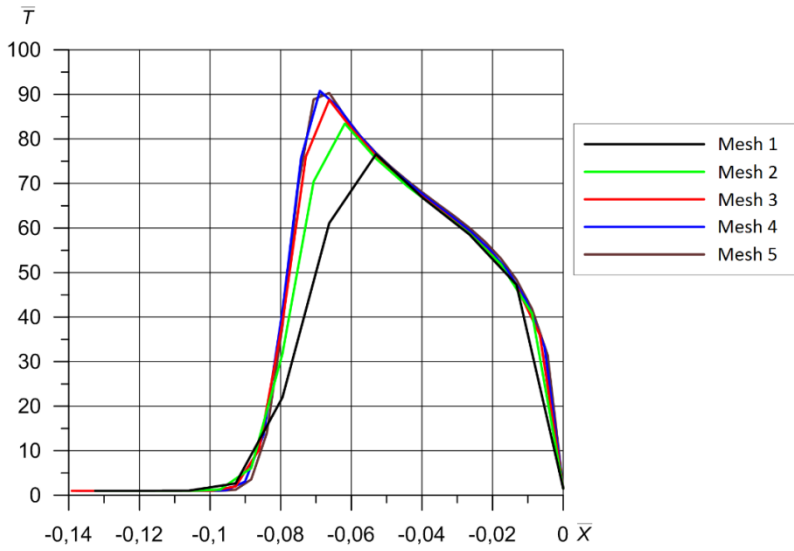


**Fig. 2.** Distribution of the dimensionless static temperature at the breaking point along the normal to the sphere surface.

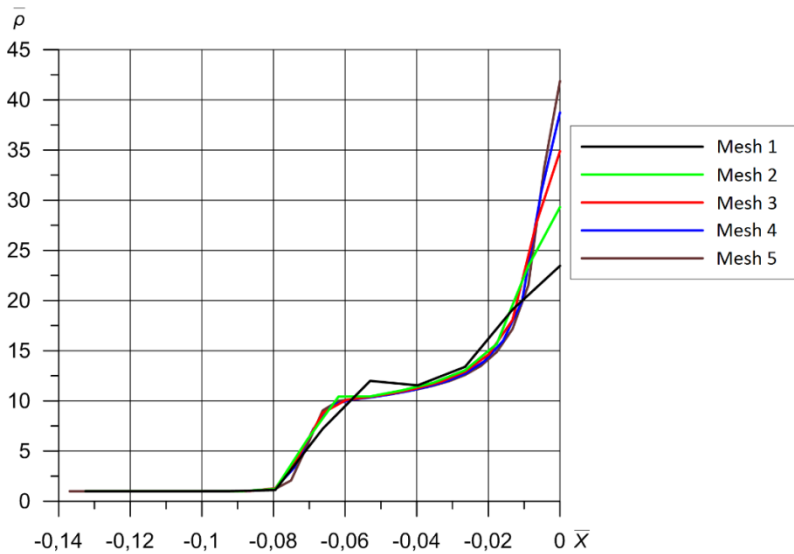


**Fig. 3.** Density distributions at the breaking point along the normal to the sphere surface.

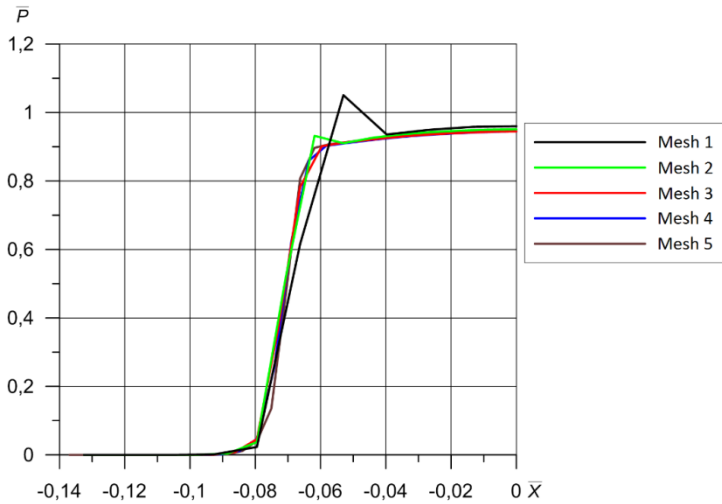


**Fig. 4.** Distribution of excess static pressure at the breaking point along the normal to the sphere surface.

Figures 2 - 4 show that the position of the shock wave and its thermodynamic parameters differ at different grid resolutions of the computational domain in the vicinity of the head compaction jump. This is explained by the fact that when using grids with finer cells, the gradients of gas-dynamic parameters are determined more reliably. It is seen that the change in the number of cells along the normal to the sphere surface affects mainly the distribution of the static temperature and its maximum value in the receding shock wave.

It is seen that the dependence tends to a certain limit, which can be considered the final solution. Note that each subsequent increase in the number of cells has less and less influence on the results obtained.

The nature of the dependence of the maximum dimensionless temperature  $\bar{T}_{\max}$  on the number of cells along the normal to the sphere surface is shown in Figure 5 (The numbers on the graph indicate the numbers of calculated grids according to Table 1). It can be seen that this dependence is limited from above by some limiting value and tends to it with an increasing number of partition cells, and each following increase in the number of cells has less influence on the value of maximum temperature.

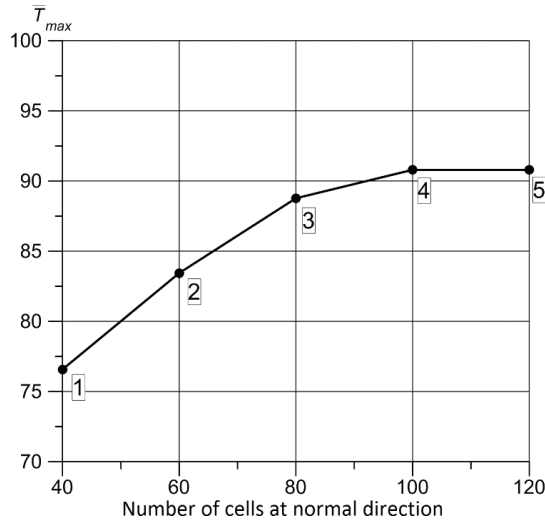


**Fig. 5.** Dependence  $\bar{T}_{max}$  of the maximum temperature in the receding shock wave on the number of cells of the partitioning of the computational domain along the normal to the sphere surface.

Figure 6 shows the dependence of the heat flux density at the front critical point on the number of cells along the normal to the sphere surface.

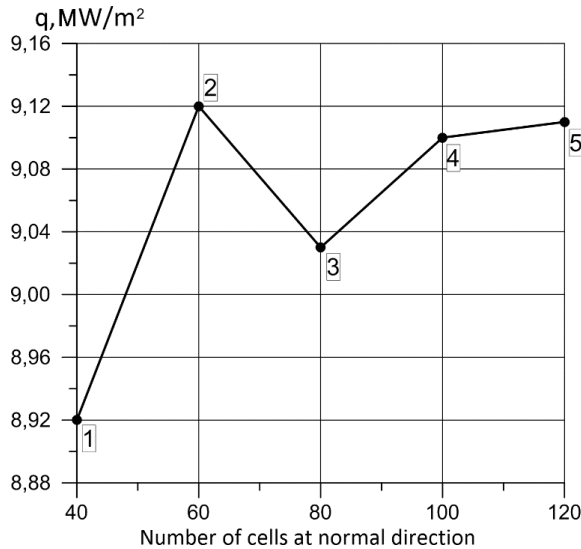


**Fig. 6.** Dependence of the heat flux density normal to the sphere surface on the number of cells partitioning the computational domain along the normal to the sphere surface.

The graph in Figure 6 shows that the dependence of the heat flux density with an increasing number of partitioning cells also tends to some limit value. The heat flux densities obtained on grids 4 and 5 differ by no more than 0.5%. However, in contrast to the dependence in Figure 5, this can be explained by a more reliable calculation of the temperature gradient not in the shock wave itself, but in the boundary layer near the sphere surface. Note the nonmonotonic nature of the dependence, which is associated with the complexity of the change in the effective thermal conductivity coefficient of a multi-

component chemically nonequilibrium gas mixture, and needs to be studied in more detail [68-70].

## 6 Conclusions

The paper analyzes the grid independence of the parameters of the high-speed flow of a mixture of gases flowing around the surface of the sphere. The dependences of the flow parameters along the normal to the sphere surface, as well as the heat flux density on the sphere surface itself, on the degree of discretization of the computational space, have been obtained. Numerical experiments have shown that with a certain number of cells the grid independence can be achieved, but the possibility of extrapolation of these data to other similar problems is not yet clear.

## References

1. L.N. Rabinskiy, S.A. Sitnikov. Development of technologies for obtaining composite material based on silicone binder for its further use in space electric rocket engines, *Periodico Tche Quimica*, 2018, 15 (Special Issue 1), p. 390–395.
2. V.A. Pogodin, L.N. Rabinskii, S.A. Sitnikov. 3D Printing of Components for the Gas-Discharge Chamber of Electric Rocket Engines, *Russian Engineering Research*. 2019. Vol. 39, No. 9. p. 797-799.
3. Formalev, V.F., Kolesnik, S.A. On Thermal Solitons during Wave Heat Transfer in Restricted Areas // *High Temperature*, 2019, 57(4), p. 498–502.
4. Radaev, S. Mathematical modeling of heat and mass transfer in heat pipes in a one-dimensional formulation when cooling active phased antenna arrays//*International Journal of Mechanics*, 2021, 15, p. 196-203.
5. Formalev, V.F., Kolesnik, S.A., Kuznetsova, E.L. Mathematical modeling of a new method of thermal protection based on the injection of special coolants // *Periodico Tche Quimica*. 2019.16(32), p. 598-607.
6. Formalev, V.F., Kartashov, É.M., Kolesnik, S.A. Simulation of Nonequilibrium Heat Transfer in an Anisotropic Semispace Under the Action of a Point Heat Source// *Journal of Engineering Physics and Thermophysics*. 2019. 92(6), p. 1537-1547.
7. Formalev, V.F., Kolesnik, S.A., Kuznetsova, E.L. Approximate analytical solution of the problem of conjugate heat transfer between the boundary layer and the anisotropic strip // *Periodico Tche Quimica*. 2019. 16 (32). p. 572-582.
8. I.S. Kurchatov, N.A. Bulychev, S.A. Kolesnik. Obtaining Spectral Characteristics of Semiconductors of AIIBVI Type Alloyed with Iron Ions Using Direct Matrix Analysis, *International Journal of Recent Technology and Engineering*, 2019, Vol. 8, I. 3, p. 8328-8330.
9. Kurchatov, I., Bulychev, N., Kolesnik, S., Muravev, E. Application of the direct matrix analysis method for calculating the parameters of the luminescence spectra of the iron ion in zinc sulfide crystals // *AIP Conference Proceedings*, 2019, 2181, 020015.
10. Kolesnik, S.A., Bulychev, N.A., Rabinskiy, L.N., Kazaryan, M.A. Mathematical modeling and experimental studies of thermal protection of composite materials under high-intensity effects of laser radiation // *Proceedings of SPIE - The International Society for Optical Engineering*. 2019. 11322,113221R.

11. Formalev, V.F., Bulychev, N.A., Kolesnik, S.A., Kazaryan, M.A. Thermal state of the package of cooled gas-dynamic microlasers //Proceedings of SPIE - The International Society for Optical Engineering. 2019. 11322,113221B.
12. Kolesnik, S.A., Bulychev, N.A. Numerical analytic method for solving the inverse coefficient problem of heat conduction in anisotropic half-space// Journal of Physics: Conference Series, 2020, 1474(1), 012024.
13. Radaev, S. Numerical and analytical modeling of permanent deformations in panels made of nanomodified carbon fiber reinforced plastic with asymmetric packing// International Journal of Mechanics, 2021, 15, p. 172-180.
14. Radaev, S. Design calculations of the limiting characteristics of heat pipes for cooling active phased antenna arrays // WSEAS Transactions on Applied and Theoretical Mechanics. 2021. 16, p. 142-149.
15. Sun, Y., Kolesnik, S.A., Kuznetsova, E.L. Mathematical modeling of coupled heat transfer on cooled gas turbine blades // INCAS Bulletin, 2020, 12 (Special Issue), p. 193–200.
16. Formalev, V.F., Kartashov, É.M., Kolesnik, S.A. On the Dynamics of Motion and Reflection of Temperature Solitons in Wave Heat Transfer in Limited Regions // Journal of Engineering Physics and Thermophysics, 2020, 93(1), p. 10–15.
17. Formalev, V.F., Bulychev, N.A., Kuznetsova, E.L., Kolesnik, S.A. The Thermal State of a Packet of Cooled Microrocket Gas-Dynamic Lasers // Technical Physics Letters, 2020, 46(3), p. 245–248.
18. O.A. Butusova. Surface Modification of Titanium Dioxide Microparticles Under Ultrasonic Treatment, International Journal of Pharmaceutical Research, 2020, Vol. 12, I. 4, pp. 2292-2296.
19. A.N. Tarasova. Vibration-based Method for Mechanochemical Coating Metallic Surfaces, International Journal of Pharmaceutical Research, 2020, Vol. 12, Supplementary Issue 2, pp. 1160-1168.
20. M.O. Kaptakov. Effect of Ultrasonic Treatment on Stability of TiO<sub>2</sub> Aqueous Dispersions in Presence of Water-Soluble Polymers, International Journal of Pharmaceutical Research, 2020, Vol. 12, Supplementary Issue 2, pp. 1821-1824.
21. O.A. Butusova. Stabilization of Carbon Microparticles by High-Molecular Surfactants, International Journal of Pharmaceutical Research, 2020, Vol. 12, Supplementary Issue 2, pp. 1147-1151.
22. M.O. Kaptakov. Catalytic Desulfuration of Oil Products under Ultrasonic Treatment, International Journal of Pharmaceutical Research, 2020, Vol. 12, Supplementary Issue 2, pp. 1838-1843.
23. A.N. Tarasova. Effect of Reagent Concentrations on Equilibria in Water-Soluble Complexes, International Journal of Pharmaceutical Research, 2020, Vol. 12, Supplementary Issue 2, pp. 1169-1172.
24. Yu.V. Ioni. Nanoparticles of noble metals on the surface of graphene flakes, Periodico Tche Quimica, 2020, Vol. 17, No. 36, pp. 1199-1211.
25. A.V. Perchenok, E.V. Suvorova, A.A. Farmakovskaya, V. Kohlert. Stabilization of aqueous dispersions of inorganic microparticles under mechanical activation, WSEAS Transactions on Applied and Theoretical Mechanics, 2021, Vol. 16, pp. 127-133.
26. N.A. Bulychev. Preparation of Stable Suspensions of ZnO Nanoparticles with Ultrasonically Assisted Low-Temperature Plasma, Nanoscience and Technology: An International Journal, 2021, Vol. 12, No. 3, pp. 91-97.

27. N.A. Bulychev. Study of Interaction of Surface-Active Polymers with ZnO Nanoparticles Synthesized in Ultrasonically Assisted Plasma Discharge, *Nanoscience and Technology: An International Journal*, 2022, Vol. 13, I. 1, pp. 55-65.
28. A.N. Tarasova. Effect of Vibration on Physical Properties of Polymeric Latexes, *International Journal of Pharmaceutical Research*, 2020, Vol. 12, Supplementary Issue 2, pp. 1173-1180.
29. M.O. Kaptakov. Enhancement of Quality of Oil Products under Ultrasonic Treatment, *International Journal of Pharmaceutical Research*, 2020, Vol. 12, Supplementary Issue 2, pp. 1851-1855.
30. Yu.V. Ioni. Synthesis of Metal Oxide Nanoparticles and Formation of Nanostructured Layers on Surfaces under Ultrasonic Vibrations, *International Journal of Pharmaceutical Research*, 2020, Vol. 12, Issue 4, pp. 3432-3435.
31. N.A. Bulychev, A.V. Ivanov. Effect of vibration on structure and properties of polymeric membranes, *International Journal of Nanotechnology*, 2019, Vol. 16, Nos. 6/7/8/9/10, pp. 334 – 343.
32. N.A. Bulychev, A.V. Ivanov. Nanostructure of Organic-Inorganic Composite Materials Based on Polymer Hydrogels, *International Journal of Nanotechnology*, 2019, Vol. 16, Nos. 6/7/8/9/10, pp. 344 – 355.
33. N.A. Bulychev, A.V. Ivanov. Study of Nanostructure of Polymer Adsorption Layers on the Particles Surface of Titanium Dioxide, *International Journal of Nanotechnology*, 2019, Vol. 16, Nos. 6/7/8/9/10, pp. 356 – 365.
34. N.A. Bulychev. Obtaining of nanosized materials in Plasma Discharges and Ultrasonic cavitation, *High Temperature*, 2021, Vol. 59, I. 4, pp. 600-633.
35. O.A. Butusova. Vinyl Ether Copolymers as Stabilizers of Carbon Black Suspensions, *International Journal of Pharmaceutical Research*, 2020, Vol. 12, Supplementary Issue 2, pp. 1152-1155.
36. A.V. Perchenok, E.V. Suvorova, A.A. Farmakovskaya, V. Kohlert. Application of vinyl ether copolymers for surface modification of carbon black, *International Journal of Circuits, Systems and Signal Processing*, 2021, Vol. 15, pp. 1414-1420.
37. O.A. Butusova. Adsorption Behaviour of Ethylhydroxyethyl Cellulose on the Surface of Microparticles of Titanium and Ferrous Oxides, *International Journal of Pharmaceutical Research*, 2020, Vol. 12, Supplementary Issue 2, pp. 1156-1159.
38. Yu.V. Ioni. Effect of Ultrasonic Treatment on Properties of Aqueous Dispersions of Inorganic and Organic Particles in Presence of Water-Soluble Polymers, *International Journal of Pharmaceutical Research*, 2020, Vol. 12, Issue 4, pp. 3440-3442.
39. N.A. Bulychev. Acoustoplasma Synthesis of Silver Nanoparticles with Antibacterial Properties, *Biophysical Journal*, 2022, Vol. 121, I. 3, Suppl. 1, p. 427a.
40. S.A. Kolesnik. Mechanical Properties of Polyethylene/Al<sub>2</sub>O<sub>3</sub> Nanoparticles Composite Material, *AIP Conference Proceedings*, 2021, Vol. 2402, article number 020026.
41. Vladimir Goncharenko, Yury Mikhaylov, Natalya Kartushina. Pattern recognition techniques for classifying aeroballistic flying vehicle paths. *Neural Computing and Applications*, 2022, Vol. 34, I. 5, pp. 4033-4045.
42. S.A. Kolesnik. Investigation of Mechanical Properties of Polymer Composite Material Based on Polyethylene with Fe<sub>2</sub>O<sub>3</sub> Nanoparticles, *AIP Conference Proceedings*, 2021, Vol. 2402, article number 020037.

43. M.O. Kaptakov, E.A. Pegachkova, A.V. Makarenko. Physical and Mechanical Properties of Composites Polyethylene – CuO Nanoparticles, AIP Conference Proceedings, 2021, Vol. 2402, article number 020038.
44. G. A. Kalugina, A. V. Ryapukhin. Impact of the 2020 Pandemic on Russian Aviation, Russian Engineering Research, vol. 41. no. 7, pp. 627-630, 2021.
45. M.O. Kaptakov. Synthesis and Characterization of Polymer Composite Materials Based on Polyethylene and CuO Nanoparticles, AIP Conference Proceedings, 2021, Vol. 2402, article number 020027.
46. Y. Burova. Concept of multistage discrete fourier transform without performing multiplications, Journal of Physics: Conference Series, 2021, vol. 1889, no. 2, 022003.
47. Astapov A.N., Pogodin V.A. Change in the integral pore size in CCCM during low-temperature oxidation // Russian Metallurgy (Metally). – 2021. – Vol. 2021, No. 12. – P. 1529 – 1533.
48. Lifanov I.P., Astapov A.N., Terentieva V.S. Deposition of heat-resistant coatings based on the ZrSi<sub>2</sub>-MoSi<sub>2</sub>-ZrB<sub>2</sub> system for protection of non-metallic composite materials in high-speed high-enthalpy gas flows // Journal of Physics: Conference Series. – 2020. – Vol. 1713, No. 1. – P. 012025.
49. Pogodin V.A., Astapov A.N., Rabinskiy L.N. CCCM specific surface estimation in process of low-temperature oxidation // Periodico Tche Quimica. – 2020. – Vol. 17, No. 34. – P. 793 – 802.
50. Yu.V. Ioni, O.A. Butusova. Preparation of Polymer Composite Material with Fe<sub>2</sub>O<sub>3</sub> Nanoparticles Synthesized with Low-Temperature Plasma under Ultrasonic Action, AIP Conference Proceedings, 2021, Vol. 2402, article number 020035.
51. Yu.V. Ioni, O.A. Butusova. Synthesis of Al<sub>2</sub>O<sub>3</sub> Nanoparticles for Their Subsequent Use as Fillers of Polymer Composite Materials, AIP Conference Proceedings, 2021, Vol. 2402, article number 020036.
52. Lifanov I.P., Yurishcheva A.A., Astapov A.N. High-temperature protective coatings on carbon composites // Russian Engineering Research. – 2019. – Vol. 39, No. 9. – P. 804 – 808.
53. Astapov A.N., Lifanov I.P., Prokofiev M.V. High-temperature interaction in the ZrSi<sub>2</sub>-ZrSiO<sub>4</sub> system and its mechanism // Russian Metallurgy (Metally). – 2019. – No. 6. – P. 640 – 646.
54. Dorrance W.H. Viscous hypersonic flow. Theory of Reacting Hypersonic Boundary Layers. Dover Publications, Inc., New York. 2017. 352 p.
55. Formalev V.F., Kolesnik S.A. Mathematical modeling of coupled heat transfer between viscous gas-dynamic flows and anisotropic bodies. (LENAND, Moscow, 2019) p. 320 [in Russian].
56. Formalev V.F., Kolesnik S.A. Conjugate heat transfer between wall gasdynamic flows and anisotropic bodies // High Temp. 2007. 45. p. 76-84.
57. Formalev V.F., Kolesnik S.A., Garibyan B.A. Analytical solution of the problem of conjugate heat transfer between a gasdynamic boundary layer and anisotropic strip // Herald of the Bauman Moscow State Technical University. Series Natural Sciences. 2020, 5(92), p. 44-59.
58. Formalev V.F., Kolesnik S.A. and Kuznetsova E.L. The effect of longitudinal nonisothermality on conjugate heat transfer between wall gasdynamic flows and blunt anisotropic bodies // High Temp. 2009. 47: 228.

59. Formalev V.F., Kolesnik S.A. and Kuznetsova E.L. Effect of Components of the Thermal Conductivity Tensor of Heat-Protection Material on the Value of Heat Fluxes from the Gasdynamic Boundary Layer // *High Temp.* 2019. 57. p. 66-71.
60. Thant Zin Hein, Boris A. Garibyan, Sergey N. Vakhneev, Olga V. Tushavina, and Vladimir F. Formalev Analytical study of joint heat transfer between a gas-dynamic boundary layer and an anisotropic strip. *INCAS bulletin.* 2020. 12, Special Issue. p. 233–243.
61. Garibyan B.A. A criterion for estimating the accuracy of numerical solutions of a nonlinear stationary heat conduction problem based on the variational principle // *Inform. and telecom. technologies.* 2019. 43. p. 6–16. [in Russian].
62. Widhopf G.F., Wang J.C.T. A TVD Finite-Volume Technique for Nonequilibrium Chemically Reacting Flows // *AIAA Paper.* 1988. 88. p. 2711.
63. Scalabrin, L.C. Numerical Simulation of Weakly Ionized Hypersonic Flow over Reentry Capsules. PhD Dissertation. University of Michigan. 2007.
64. Bonnie J. McBride, Dr. Michael J. Zehe, Gordon S. NASA Glenn Coefficients for Calculating Thermodynamic Properties of Individual Species. – National Aeronautics and Space Administration John H. Glenn Research Center at Lewis Field Cleveland, 2002. 291 p.
65. Millat, J., Dymond, J. H. and Nieto de Castro, C. A. Transport Properties of Fluids: Their Correlation, Prediction and Estimation, Cambridge University Press. 1996.
66. Blottner F. G., Johnson M., Ellis M. Chemically reacting viscous flow program for multi-component gas mixtures // SC-RR-70-754, Sandia Laboratories, Albuquerque, New Mexico, 1971.
67. Landau L.D., Lifshitz E.M. *Statistical Physics*, 3d Edition, Pergamon Press. 1980. 562 p.
68. N.A. Bulychev. Obtaining of Gaseous Hydrogen and Silver Nanoparticles by Decomposition of Hydrocarbons in Ultrasonically Stimulated Low-Temperature Plasma, *International Journal of Hydrogen Energy*, 2022, Vol. 47, I. 50, pp. 21323-21328.
69. N.A. Bulychev, A.Yu. Burova. Unerroric of control of mutual compliance of the efficiency of hydrogen engines of unmanned vehicles in the conditions of mass production, *International Journal of Hydrogen Energy*, 2022, Vol. 47, I. 63, pp. 26789-26797.
70. N.A. Bulychev. Synthesis of Gaseous Hydrogen and Nanoparticles of Silicon and Silica by Pyrolysis of Tetraethoxysilane in an Electric Discharge under the Ultrasonic Action, *International Journal of Hydrogen Energy*, 2022, Vol. 47, I. 84, pp. 35581-35587.